Opening of nucleic-acid double strands by helicases: Active versus passive opening

M. D. Betterton
Department of Applied Mathematics, University of Colorado at Boulder, 526 UCB, Boulder, Colorado 80309, USA

Frank Jülicher
Institut Curie, Max-Planck Institute for the Physics of Complex Systems, Nöthnitzerstrasse 38, 01187 Dresden, Germany
(Received 3 September 2004; published 19 January 2005)

Helicase proteins move along double-stranded nucleic-acid molecules and unwind the double helix. This paper presents a theoretical study of the coupling between helicase translocation and duplex unwinding. Two different cases—active and passive opening—are usually distinguished. In active opening, the helicase directly destabilizes the double-stranded nucleic acid (dsNA) to promote opening. Passive opening implies that the helicase binds ssNA available when a thermal fluctuation partially opens the dsNA. We formulate a discrete model for helicase motion. An interaction potential describes how the helicase affects duplex unwinding when near a junction between single-stranded and double-stranded NA. Different choices of the potential correspond to the cases of active and passive opening. An optimal choice of interaction potential leads to a helicase which can *unwind* NA as rapidly as it *translocates* on single strands.

DOI: 10.1103/PhysRevE.71.011904 PACS number(s): 82.39.−k, 87.10.+e, 05.40.−a, 82.20.−w

I. INTRODUCTION

Helicases are motor proteins which open double-stranded nucleic-acid (NA) molecules. The strand separation is fueled by nucleotide triphosphate (NTP) hydrolysis, typically of ATP. Helicases play a role in nearly every cellular process which involves NA, including DNA replication, transcription, translation, repair, and RNA processing [1]. All helicases move along NA strands and couple motion to strand separation. For this reason, helicases are also NA translocases [2,3].

In this work we discuss unwinding by helicases which translocate directionally on single-stranded (ss) NA. Such a description is particularly relevant to the superfamily I and II (SF1 and SF2) helicases, many of which translocate on ssNA [3]. Upon reaching the ss–double-strand (ds) junction, the helicase moves the junction forward, creating additional ssNA "track" (Fig. 1). We consider how a helicase may efficiently couple ss translocation to unwinding. In the experimental literature on helicases, this coupling is classified as passive or active [1–3]. A passive helicase waits for a thermal fluctuation that opens part of the dsNA, and then moves forward and binds to the newly available ssNA. An active helicase directly destabilizes the dsNA, presumably by changing the free energy of the ds state. In this paper, we describe the principles of this process and show how an optimal choice of interaction maximizes the unwinding rate.

Experiments on the SF1 protein PcrA have been proposed to demonstrate that this helicase unwinds actively. In a crystallographic study, Velankar *et al.* observed that certain portions of PcrA protein appeared to interact with and distort duplex DNA in cocrystals of PcrA and DNA [4]. When these specific portions of the protein were altered, the mutant proteins unwound dsDNA 10–30 times more slowly than the wild-type protein (depending on which residue was mutated). However, the mutant ATPase activity on single strands was unchanged, suggesting the mutant helicases maintained wild-type ssNA translocation activity [5].

Helicases are an important class of enzymes which interact with NA, yet have many relatively simple features. For example, many helicases unwind NA at rates which are independent of the NA sequence, within experimental resolution [1,6–9]. Thus, the information content of the NA is apparently not essential to helicase operation—a large simplification compared to RNA polymerases, for example [10,11].

Although extensive biochemical and structural studies of helicases have been performed, few mathematical models of helicases have been studied. Work includes a "flashing-field" model specific to hexameric ring helicases [12], a description of a helicase as a biased random walk, which considered how the density of histones affects the random walk [13], and a phase-coexistence model of ss and dsDNA in the presence of a helicase [14]. Recently, a physical description of helicase unwinding of NA has been proposed which contains both active and passive opening as different cases in a general framework [15]. Here we extend this study, fully describe the solutions, and discuss the consequences for NA unwinding.

An important property of NA is the thermally activated opening and closing of double strands. Although thermal fluctuations open the dsNA, under typical conditions it is thermodynamically stable and on average closes. For unwinding to occur, the helicase and the NA ss-ds junction

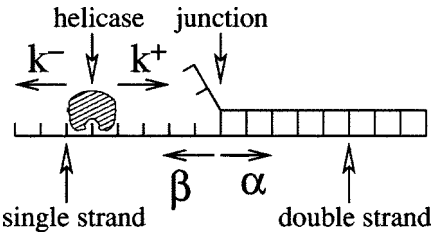

FIG. 1. Sketch of helicase on NA. The helicase moves forward (toward the dsNA) at rate k^+ and backward at rate k^-. The NA opens at rate α and closes at rate β.

must interact. An interaction potential describes how the presence of the helicase modifies NA opening. Passive opening corresponds to a hard-wall potential: the helicase inhibits NA closing, but does not otherwise affect the dsNA. A softer potential corresponds to active opening. We calculate exactly the unwinding rate for different interaction potentials. Passive unwinding is slower than one simple type of active opening. The interaction potential can be chosen to maximize the unwinding rate, and we show that an optimized active helicase can unwind dsNA as fast as it translocates on ssNA.

II. DISCRETE MODEL FOR NA UNWINDING

A. NA opening

Before discussing helicase-driven unwinding of NA, we describe the properties of NA and helicase when the helicase is far from the single-strand–double-strand (ss-ds) fork on the ssNA. The dsNA opens and closes due to thermal fluctuations. We describe thermal breathing by the rates α and β at which the NA base pair at the ss-ds junction opens and closes, respectively. For simplicity, we assume that these rates are independent of the NA base sequence. Because the NA tends to close, we have $\beta > \alpha$ (in the absence of melting agents [2]). Here, we consider fluctuations for which the NA opens or closes at the ss-ds fork only. We thus ignore fluctuations where the dsNA opens spontaneously and forms a bubble surrounded by dsNA. Modes where few or many bases open within the dsNA exist, but when the NA is well below the melting temperature they are rare and can be neglected.

Since the NA breathing results from thermal fluctuations, the rates α and β satisfy detailed balance:

$$\frac{\alpha}{\beta} = e^{-\Delta G}, \tag{1}$$

where ΔG is the free energy of one base-pair bond. Throughout this paper, we write energies in units of $k_B T$ (T is temperature and k_B the Boltzmann constant). We ignore sequence effects on the fluctuations of NA opening, average over sequence inhomogeneities, and estimate $\Delta G \approx 2$ for a base pair near a junction [16]. This value is consistent with bulk melting-curve results [1]. Thus we estimate $\alpha/\beta \approx e^{-2} \approx 1/7$. To date, α and β have not been directly measured. In Appendix A we estimate $\alpha \approx 10^7\ \mathrm{s}^{-1}$ from experiments which measure the opening rate of short DNA hairpins.

B. Helicase translocation on single strands

If the helicase is far from the ss-ds junction on the single strand, it advances on the ssNA in a given direction (Fig. 1). We denote the rate of motion toward the ss-ds junction by k^+, and the backward rate by k^-. We assume here that the helicase moves in single-base steps. (Note that a helicase might take steps of several bases on ssNA. In this case we can adapt the step size in our description.) The helicase transduces the chemical energy of ATP hydrolysis to generate directed motion with $k^+ \gg k^-$. Directed motion is possible because the single strand is asymmetric with two different ends, the $3'$ and $5'$ ends. In some cases we neglect backward steps and assume $k^- \approx 0$ even though in general $k^- > 0$.

Helicase motion is a nonequilibrium process because it is driven by ATP hydrolysis. The rates k^+ and k^- do not correspond to thermal transitions and therefore do not satisfy detailed balance. These rates are instead determined by the mechanochemical coupling of ATP hydrolysis to motion. In Appendix B we discuss a simple model for motion generation driven by ATP hydrolysis. This model determines the rates k^+ and k^- which result ultimately from conformational changes of the protein; we give explicit expressions for k^+ and k^- in different regimes.

C. Interaction potential

Helicase-catalyzed unwinding of NA requires an interaction between the helicase and the ss-ds junction. Suppose the helicase is bound at base n along the NA strand and the NA ss-ds junction is at base m (Fig. 1). Since the helicase moves forward (increasing n) and the NA tends to close (decreasing m), the motion of the helicase and junction tend to drive their positions closer together. When the helicase and the NA ss-ds junction are close to each other, they interact. We describe the interaction by a potential $U(m-n)$ which depends only on the difference $j=m-n$. For large separations $j \gg 1$ the junction and the helicase have no effect on each other, so the coupling potential tends to zero. In this limit the helicase ss translocation and the DNA fluctuations are decoupled. However, when j is small the coupling potential changes both helicase and junction motion: $U>0$ inhibits the forward motion of the helicase and increases the relative opening rate of the junction.

Detailed balance determines how the coupling potential changes the NA opening and closing rates. If the NA closes ($m \to m-1$), the interaction energy changes from $U(j)$ to $U(j-1)$. The ratio of β_j to α_{j-1} therefore satisfies

$$\frac{\beta_j}{\alpha_{j-1}} = \frac{\beta}{\alpha} e^{-[U(j-1)-U(j)]}, \tag{2}$$

where α and β are the rates in the limit $j \to \infty$ where the helicase and junction are well separated. Here the subscript denotes the helicase-junction separation before the opening or closing occurs.

The potential also influences helicase translocation. The change in energy $U(j-1)-U(j)$ characterizes the effective force acting on the helicase. Since the helicase hydrolyzes ATP and its motion is a nonequilibrium phenomenon, detailed balance does not apply. In Appendix B we present a simple two-state model for nonequilibrium helicase translocation. While in general the forward and backward rates have a complex dependence on external force, there are simple limits which are convenient for our discussion. In particular, the ratio of the rates satisfies an exponential, detailed-balance-like relation in many situations where ATP hydrolysis is tightly coupled to motion. In this case, the ratio satisfies

$$\frac{k_j^+}{k_{j-1}^-} \simeq \frac{k^+}{k^-} e^{-[U(j-1)-U(j)]}. \tag{3}$$

We use this simple relation to illustrate the principles of helicase motion which do not depend in detail on the force dependence of the hopping rates.

Equations (2) and (3) determine only the ratios of the rates. The energy barrier to single-base steps of the helicase or junction determines how the individual rates change. The effect of the energy barrier on the rates can be represented by a coefficient $0<f<1$:

$$k_j^+ = k^+ e^{-f[U(j-1)-U(j)]},$$

$$k_{j-1}^- = k^- e^{-(f-1)[U(j-1)-U(j)]},$$

$$\beta_j = \beta e^{-f[U(j-1)-U(j)]},$$

$$\alpha_{j-1} = \alpha e^{-(f-1)[U(j-1)-U(j)]}. \tag{4}$$

Smaller values of f imply that the potential changes predominantly the backward rates, while for large f the interaction primarily affects the forward rates. Note that we assume for simplicity that the interaction energy only depends on the separation between the helicase and junction. Therefore, changing the separation either by NA breathing or by helicase motion changes the energy in the same way. In other words, f is the same for the helicase motion and the NA breathing since both phenomena involve the same barrier. We emphasize that $f=0$ and $f=1$ are physically unrealistic and singular limits.

We do not know *a priori* the shape of the coupling potential $U(j)$. In Sec. III below, we study different forms of $U(m-n)$ subject to the requirements (i) $U\to 0$ for $m \gg n$ (when the helicase and the junction are far apart, there is no interaction) and (ii) $U\to\infty$ for $n \gg m$. The second requirement implies that the helicase remains near the ssNA—for example, because it cannot move solely on dsNA. This increase in U is necessary to confine the helicase near the ss-ds junction.

D. Solving for the opening rates

Given the rates k^+, k^-, α, and β, the coupling potential $U(m-n)$, and the parameter f, we can determine the mean rate of dsNA unwinding and the diffusion coefficient for fluctuations about the mean. Consider the probability $P(n,m,t)$ that the helicase is at position n and the ss-ds junction is at position m at time t. The probability function is non-negative with $\Sigma_{n,m}P(n,m,t)=1$ for all t. The dynamics of P are described by

$$\begin{aligned}\frac{dP(n,m)}{dt} &= -(\alpha_{m-n}+\beta_{m-n}+k^+_{m-n}+k^-_{m-n})P(n,m)\\ &+ \alpha_{m-n-1}P(n,m-1)+\beta_{m-n+1}P(n,m+1)\\ &+ k^+_{m-n+1}P(n-1,m)+k^-_{m-n-1}P(n+1,m).\end{aligned} \tag{5}$$

This equation describes the changes to $P(n,m,t)$ due to opening and closing of the NA (which change m) and helicase steps (which change n). We rewrite using the difference $j=m-n$ and midpoint $l=m+n$:

$$\begin{aligned}\frac{dP(j,l)}{dt} &= -(\alpha_j+\beta_j+k_j^++k_j^-)P(j,l)+\alpha_{j-1}P(j-1,l-1)\\ &+ \beta_{j+1}P(j+1,l+1)+k_{j+1}^+P(j+1,l-1)\\ &+ k_{j-1}^-P(j-1,l+1).\end{aligned} \tag{6}$$

Since the coefficients in Eq. (6) are independent of l, we can sum over l to obtain an equation for the difference-variable distribution $\mathcal{P}_j=\Sigma_l P(j,l)$:

$$\begin{aligned}\frac{d\mathcal{P}_j}{dt} &= -(\alpha_j+\beta_j+k_j^++k_j^-)\mathcal{P}_j+(k_{j-1}^-+\alpha_{j-1})\mathcal{P}_{j-1}\\ &+ (k_{j+1}^++\beta_{j+1})\mathcal{P}_{j+1}.\end{aligned} \tag{7}$$

This equation describes transitions that increase j at rate $k_j^-+\alpha_j$ and transitions that decrease j at rate $k_j^++\beta_j$. The difference-variable probability distribution $\mathcal{P}_j$ relaxes to a steady state in finite time while the motion in the midpoint variable l undergoes drift with diffusion. Since the NA opening and closing times are of the order of microseconds, we expect that $\mathcal{P}_j$ rapidly relaxes to the stationary distribution satisfying

$$I(j)=I(j-1), \tag{8}$$

where the flux of probability between j and $j+1$ is

$$I(j)=(\alpha_j+k_j^-)\mathcal{P}_j-(\beta_{j+1}+k_{j+1}^+)\mathcal{P}_{j+1}. \tag{9}$$

The stationary distribution for j thus corresponds to constant probability flux. Because $U(j)\to\infty$ as $j\to-\infty$, this flux must be zero (no probability can escape to $j\to-\infty$). Setting Eq. (9) $=0$ gives a recursion relation for $\mathcal{P}_j$:

$$\mathcal{P}_{j+1}=\frac{\alpha_j+k_j^-}{\beta_{j+1}+k_{j+1}^+}\mathcal{P}_j. \tag{10}$$

The rates k_j^+, k_j^-, α_j, and β_j are determined by the coupling potential, and therefore $\mathcal{P}_j$ depends on $U(j)$.

For times long compared to the relaxation time of the difference variable, fluctuations in j and l become independent. In this limit, we can write $P(j,l)=\mathcal{P}_j\Pi_l$, where Π_l is the probability distribution in l. We substitute this expression in Eq. (6) and define

$$p=\sum_j(\alpha_j+k_j^+)\mathcal{P}_j, \tag{11}$$

$$q=\sum_j(\beta_j+k_j^-)\mathcal{P}_j. \tag{12}$$

We find an equation for Π_l:

$$\frac{d\Pi_l}{dt}=-(p+q)\Pi_l+p\Pi_{l-1}+q\Pi_{l+1}. \tag{13}$$

The dynamics in the midpoint variable l are a combination of drift (if $p\neq q$) and diffusion. As above, we define the current in the variable l:

$$\Upsilon(l) = p\Pi_l - q\Pi_{l+1}. \tag{14}$$

Thus the equation for the stationary distribution Π_l is

$$\Upsilon(l) = \Upsilon(l-1). \tag{15}$$

The rates p and q are independent of l, because the rates depend only on the difference variable j. Therefore the dynamics in l are translationally invariant. The steady-state solution is a constant (independent of l). We have $\Pi_0 = 1/N$ and $\Upsilon = (p-q)\Pi_0$, where N is the total number of NA bases. The mean unwinding rate of a single helicase is therefore

$$v = \frac{1}{2}(p-q) = \frac{1}{2}\sum_j (k_j^+ + \alpha_j - k_j^- - \beta_j)\mathcal{P}_j. \tag{16}$$

The factor of $1/2$ appears because we use $l=m+n$, while the true midpoint location is $l/2$. The expression for v has a simple physical interpretation. The quantity in parentheses is the net unwinding rate at separation j. A forward hop of the helicase (k_j^+) or NA opening (α_j) moves the helicase-junction complex forward. Similarly, a backward hop of the helicase (k_j^-) or NA closing (β_j) moves the complex backward. We multiply the unwinding velocity at separation j by the probability $\mathcal{P}_j$ of finding the complex at separation j. Repeating this addition for all possible j, we arrive at Eq. (16). Thus solving Eq. (10) for $\mathcal{P}_j$ immediately gives the mean helicase unwinding rate.

To find the effective diffusion coefficient which describes the fluctuations about the mean unwinding rate, we consider the decay rate of modes with wave number λ. For the ansatz $\Pi_l = \Pi_\lambda e^{i\lambda l} e^{-t/\tau + i\omega t}$ we have

$$\frac{1}{\tau} - i\omega = (p+q) - pe^{-i\lambda} - qe^{i\lambda}. \tag{17}$$

In the limit of long wavelength (small λ), this becomes

$$\frac{1}{\tau} - i\omega = -2iv + 4D\lambda^2 + \mathcal{O}(\lambda^4), \tag{18}$$

where v is the velocity. The diffusion coefficient which characterizes velocity fluctuations is thus

$$D = \frac{1}{4}(p+q) = \frac{1}{4}\sum_j (k_j^+ + \alpha_j + k_j^- + \beta_j)\mathcal{P}_j. \tag{19}$$

III. PASSIVE VERSUS ACTIVE UNWINDING

In this section we study helicase unwinding for specific coupling potential shapes (Fig. 2). The hard-wall and staircase potentials give a simple representation of passive and active opening, respectively. We also examine the case where the interaction between helicase and junction hinders unwinding. These results let us compare the basic properties of passive and active opening.

A. Passive unwinding

The term "passive" is typically used for a helicase which inhibits NA closing (when near the ss-ds junction) but does not enzymatically accelerate NA opening [1–3]. In this picture, the helicase translocates on ssNA toward the ss-ds junction. Once the helicase reaches the junction, it can only advance if a fluctuation opens the adjacent NA base pair. The helicase then translocates forward by one base and blocks closing of the newly opened base pair. We can describe this regime with an appropriate interaction potential $U(m-n)$. We will find that the base pair adjacent to the helicase has a probability α/β of being open. Thus, when the helicase attempts a forward hop it succeeds with probability α/β.

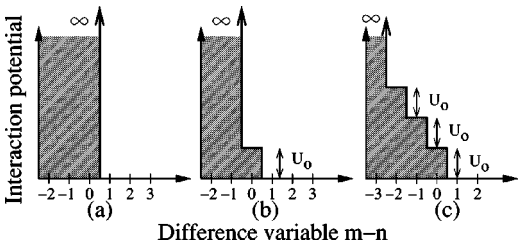

FIG. 2. Coupling potentials between the helicase and ss-ds junction. (a) Hard-wall potential corresponding to passive opening. (b) A potential with a step, which corresponds to active opening. (c) Three-step staircase potential.

We suppose that the helicase-dependent inhibition of NA closing requires the helicase to be adjacent to the junction: when the junction is at position $m=n+1$, the helicase covers the ss base nearest the junction and prevents base pairing with the complementary NA strand. Thus passive opening requires $\beta_1 = 0$. By comparison to Eq. (2), we see that $\beta_1 = 0$ if $U(0)$ is infinite. This is the hard-wall potential sketched in Fig. 2(a). The potential affects the helicase motion according to Eq. (3): if $U(0)$ is infinite, then $k_1^+ = 0$. Thus the helicase at $n=m-1$ is unable to advance into the dsNA until a fluctuation opens the NA. The hard-wall coupling potential thus prevents overlap of the helicase and the dsNA.

For a hard-wall potential, k^+, k^-, α, and β are constant in the region $j>0$ except at $j=1$, where $k_1^+ = \beta_1 = 0$. Since the rates are constant, we have

$$\mathcal{P}_j = A\left(\frac{\alpha + k^-}{\beta + k^+}\right)^j = Ac^j, \tag{20}$$

where we have defined $c = (\alpha + k^-)/(\beta + k^+)$ and the constant A is determined from normalization:

$$A = \frac{\beta + k^- - \alpha - k^-}{\alpha + k^+}. \tag{21}$$

Evaluating Eq. (16) for the mean unwinding rate we find

$$v_{HW} = \frac{\alpha k^+ - \beta k^-}{\beta + k^+}. \tag{22}$$

The unwinding velocity is positive when $k^+/k^- > \beta/\alpha$. That is, the free-energy change of closing one NA base must be smaller than the effective free-energy change driving the helicase. This requirement implies that the energy supplied by ATP hydrolysis must exceed the energy required to separate the NA strands.

The maximum v_{HW} occurs when $k^-=0$; fastest unwinding occurs for a unidirectional helicase. This upper bound is

$$v_{HW}^{\max}=\frac{\alpha}{\beta}\left(\frac{k^+}{1+k^+/\beta}\right)\approx\frac{\alpha}{\beta}k^+, \tag{23}$$

where we have assumed that $k^+\ll\beta$. Thus a passive helicase unwinds more slowly than it translocates on ssNA by a factor $\approx\alpha/\beta$. This result has a simple interpretation: the base pair adjacent to the helicase has a probability α/β of being open. Thus, when the helicase attempts a forward hop it succeeds with probability α/β.

B. Active opening: The step potential

A coupling potential $U(j)$ with nonzero range corresponds to active unwinding and leads to position-dependent rates given by Eq. (4). Whenever NA closing increases the interaction energy, so that $U(j-1)>U(j)$, the ratio $\beta_j/\alpha_{j-1}<\beta/\alpha$. Thus a repulsive coupling potential between the NA and helicase can increase the rate of opening, decrease the rate of closing, or both.

Consider a coupling potential with a step of height $U_0=U(0)-U(1)$ at $j=0$ and a hard wall at $j=-1$ [Fig. 2(b)]. The dsNA and helicase can overlap by one base if the energetic cost U_0 is paid. At the step we have

$$\frac{k_0^-}{k_1^+}=\frac{k^-}{k^+}e^{U_0},$$

$$\frac{\alpha_0}{\beta_1}=\frac{\alpha}{\beta}e^{U_0},$$

$$k_0^+=\beta_0=0. \tag{24}$$

The individual rates are, as above,

$$k_1^+=k^+e^{-fU_0},$$

$$k_0^-=k^-e^{-(f-1)U_0},$$

$$\beta_1=\beta e^{-fU_0},$$

$$\alpha_0=\alpha e^{-(f-1)U_0}. \tag{25}$$

Using these expressions, the steady-state difference-variable probability distribution is

$$\mathcal{P}_j=\begin{cases}Ae^{-U_0}c^{-1}, & j=0,\\ Ac^{j-1}, & j>0,\end{cases} \tag{26}$$

where $c=(\alpha+k^-)/(\beta+k^+)$ and A is a normalization constant. The unwinding velocity v_1 for a one-step potential, relative to v_{HW} of Eq. (22), is

$$\frac{v_1}{v_{HW}}=\frac{c+(1-c)e^{-fU_0}}{c+(1-c)e^{-U_0}}. \tag{27}$$

The ratio v_1/v_{HW} depends strongly on f (Fig. 3). For small values of f the helicase forward rate k^+ and the DNA closing rate β do not change much due to the step, while the helicase backward rate k^- and the DNA opening rate α increase significantly. Our result shows that to accelerate unwinding, it is better to increase α than to decrease β, because faster opening increases the strand-separation time scale. In particular, from Eq. (27) we see that in the limit $f\to 0$ and $U_0\gg 1$, $v_1\to v_{HW}/c$. Recall that the maximal unwinding rate for passive opening is approximately a factor of c smaller than the helicase ss translocation rate. Active unwinding with small f can increase the unwinding rate by c^{-1}. In other words, such a helicase can unwind dsNA as fast as it translocates on single strands.

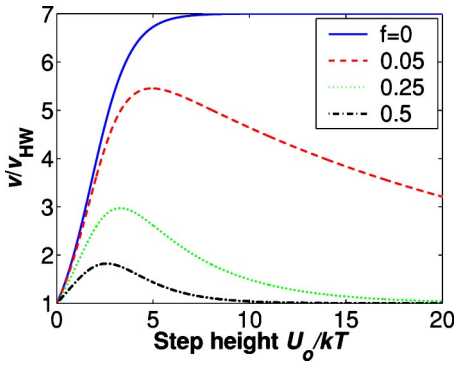

FIG. 3. Unwinding rate (relative to the hard-wall rate) for a one-step potential as a function of step height. The different curves correspond to different values of the parameter f. The maximum opening speed increases for small f (see text).

The step height U_0 significantly affects the unwinding rate. For small U_0, v_1 is comparable to v_{HW}. As the step height increases, v_1 increases, because the step increases the NA opening rate α_0. For $U_0=1$ and $f=0.05$, the unwinding rate is approximately twice the hard-wall velocity. For larger U_0, the unwinding rate reaches a maximum and begins to decrease. The decrease for large U_0 occurs when the helicase backward rate k_0^- is significantly increased by the step.

C. Active opening: The staircase potential

Known helicase proteins are large compared to the size of one NA base [1]. Thus the coupling potential may extend the helicase-junction interaction over multiple bases. Here we consider a staircase potential with n identical steps, each of height U_0 (Fig. 2(c)). The potential has a wall ($U\to\infty$) at $j=-n$. The steady-state difference-variable probability distribution is

$$\mathcal{P}_j=\begin{cases}Ae^{(j-1)U_0}c^{j-1}, & -n+1\leqslant j\leqslant 0,\\ Ac^{j-1}, & j>0,\end{cases} \tag{28}$$

where A is determined by $\Sigma_j\mathcal{P}_j=1$. The unwinding velocity is, for $n\gg 1$,

$$\frac{v_n}{v_{HW}}=\frac{c^n+(1-c)e^{-(f-1)U_0}\sum_{j=1}^{n}c^{n-j}e^{-jU_0}}{c^n+(1-c)\sum_{j=1}^{n}c^{n-j}e^{-jU_0}},$$

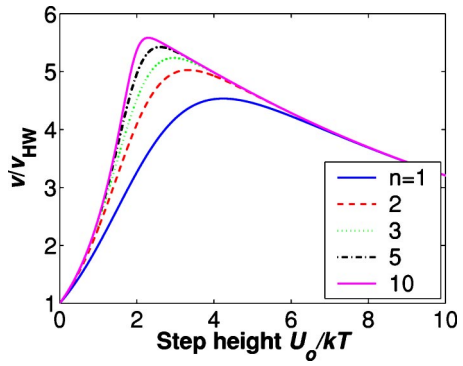

FIG. 4. Unwinding rate (relative to the hard-wall rate) as a function of step height, shown for staircase potentials with different number of steps. The parameter $f=0.05$.

$$= \frac{c^n(e^{-U_0}-c)+e^{-fU_0}(1-c)(e^{-nU_0}-c)}{c^n(e^{-U_0}-c)+e^{-U_0}(1-c)(e^{-nU_0}-c)}. \tag{29}$$

Note that for $n=1$ this expression reduces to Eq. (27). In the special case $n=0$ the sums are absent. In this case, we recover the hard-wall case with $v_0/v_{HW}=1$. In Fig. 4 we show how the unwinding rate varies with the number of steps. As n increases, the unwinding velocity grows more quickly for small U_0. The maximum opening rate also increases. For one step with $U_0=2$, the unwinding velocity is three times the hard-wall rate, whereas for five steps of height 2 the opening velocity is 5 times the hard-wall velocity ($f=0.05$). This is a significant increase over the hard-wall velocity. At best, a helicase with a staircase potential can unwind NA as fast as it translocates on ssNA.

D. Maximizing the unwinding rate

If rapid unwinding is advantageous, helicases will evolve toward coupling potentials which maximize the unwinding rate. This question can be addressed systematically by first looking at the limit of a large number of steps in the staircase potential ($n\to\infty$). In this case, the step size U_0 corresponding to the maximum opening velocity approaches $U_{max}\approx -\ln c$. Recalling that $c\approx\alpha/\beta=e^{-\Delta G}$, we see that, in the limit of a large number of steps,

$$U_{max}\approx\Delta G. \tag{30}$$

Thus the optimal step height for rapid unwinding approaches the free-energy change of melting one base of NA. This result reflects the trade-off inherent in the choice of a coupling potential: an increase in the step height U_0 means that for small j the NA opening rate increases and the helicase forward rate decreases. In practice, the limiting value $U_{max}\approx\Delta G$ is a good approximation for as few as five steps in the potential (Fig. 4).

E. Negative staircase potential

In general, the step height of the potential could also be negative, which corresponds to an attractive interaction between the helicase and junction. Then the potential hinders unwinding because it accelerates closing of the NA. In this case, the curves for potentials with a varying number of identical steps are similar. If we define $W=-U_0>0$, then for all n, Eq. (29) is well approximated by

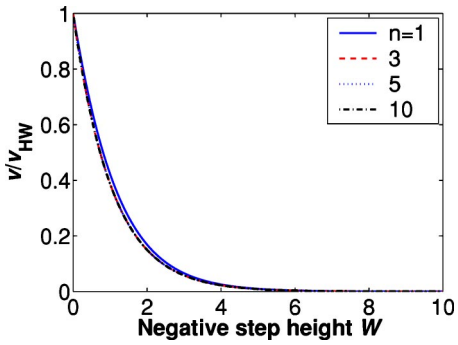

FIG. 5. Unwinding rate (relative to the hard-wall rate) as a function of step depth, shown for negative staircase potentials with different number of steps. Here $f=0.05$.

$$\frac{v_n}{v_{HW}}\approx e^{-(1-f)W}. \tag{31}$$

Thus a negative staircase leads to an exponentially decreasing unwinding rate below the hard-wall value. In Fig. 5 we show the decrease in unwinding rate for this worse-than-passive helicase. For $W=2$, the unwinding rate is approximately 5 times slower than the passive helicase ($f=0.05$).

IV. DISCUSSION

We have described the opening of NA by a helicase in terms of two degrees of freedom: the position of the helicase, which moves along ssNA driven by ATP hydrolysis, and the position of the ss-ds NA junction, which undergoes thermal fluctuations and closes (on average) if a helicase is not present. This simple model allows us to focus on how the motion is affected by the helicase-junction interaction. We show that the interaction between helicase and dsNA determines the rate of unwinding; active opening in general leads to a faster unwinding rate that can approach the rate of helicase motion along the ssNA.

This approach is similar to the polymerization ratchet of Peskin, Odell, and Oster, who examined how a polymerizing filament is able to produce a force [17]. In their work, the two fluctuating degrees of freedom are the tip of a filament and a wall, which are analogous to our helicase and ss-ds junction. They considered a hard-wall interaction; thus our work is a generalization of their approach.

The hopping rates k^+ and k^- are difficult to measure experimentally. Experiments on ss translocation provide a value for the difference k^+-k^-. Such measurements, however, do not measure the individual rates. In single-molecule experiments, the average single-strand translocation rate could be directly observed (although to our knowledge, no such experiments have yet been published). Carefully designed bulk experiments can also measure single-strand translocation. Bulk data on ss translocation have been published for two helicases: work by Dillingham, Wigley, and Webb examined PcrA helicase [6,18], while Kim, Narayan,

and Patel studied T7 DNA helicase [19]. The data of Dillingham *et al.* are particularly useful in our discussion, because PcrA helicase is believed to take single-base steps on ssNA. Assuming a single population of helicases, they found $k^+ - k^- = 80$ bases s^{-1}. As discussed above, $\beta/\alpha \approx 7$ for DNA. Thus, for unwinding to be possible, as shown in Eq. (22), we must have $k^+ > 7k^-$. This result is consistent with the experiments of Dillingham *et al.*: their data were well fit by a model with no backward steps ($k^- = 0$), although our analysis of their results found a comparably good fit with values of k^- up to 10% of k^+.

Using these experimental values, for PcrA the maximum possible hard-wall unwinding velocity [Eq. (23)] is

$$v_{HW} = \frac{\alpha}{\beta}\left(\frac{k^+}{1 + k^+/\beta}\right) \approx 11 \text{ bp s}^{-1}. \tag{32}$$

By contrast, if PcrA has optimized its coupling potential for rapid opening, the unwinding velocity is approximately equal to the ss translocation rate. The maximum unwinding rate of PcrA is therefore 80 bp s^{-1} (under the same experimental conditions as the measurement of ss translocation).

To our knowledge, a direct comparison between the rate of ss translocation and ds unwinding has not been performed for any helicase. Typical unwinding assays are indirect: they use gel electrophoresis to determine the fraction of dsNA molecules completely unwound at a given time [1,5]. A number of single-molecule experiments have directly measured helicase unwinding rates [7–9,20,21]. However, ss translocation for the same helicases has not been measured. (In fact, several of the single-molecule studies used the helicase RecBCD [7–9], which is believed not to translocate on ssNA [1].) We anticipate that future experiments on helicases will measure both translocation and unwinding rates, enabling a direct test of our model.

Although the unwinding rate has not been directly measured, a comparison of active versus passive opening for PcrA has been suggested. Velanakar *et al.* crystallized PcrA protein with a forked (part ss and part ds) DNA substrate [4]. In the crystal structure, certain parts of PcrA appear to bind the dsDNA and distort the double helix. In a follow-up study, researchers from the same laboratory introduced mutations to the PcrA residues which appear to interact with dsDNA in the crystal structure [5]. The mutant proteins showed ATP hydrolysis activity in the presence of ssDNA similar to the wild-type protein, suggesting that the mutant helicases had no defect in ssDNA translocation. However, the altered proteins unwound dsDNA 10–30 times more slowly than the wild-type protein (depending on which residue was mutated). These experiments suggest that PcrA unwinds actively and that passive unwinding may be slower and less effective than active. In the language of our model, the mutations may alter the potential so it approaches a hard-wall or negative-staircase form (corresponding to passive or worse-than-passive opening). The results of our model demonstrate striking quantitative agreement with the results on PcrA: changing an optimized, active helicase to a passive form decreases the unwinding rate by a factor of $c^{-1} \approx 7$. Further altering the potential to a negative staircase with a well depth of $2k_BT$ decreases the unwinding rate by a factor of 35. Despite the simplicity of our model, we find that small changes to the coupling potential cause the unwinding rate to vary by a large factor.

We emphasize that changes to the helicase hopping rates k^+ and k^-—for example, due to changes in the ATP concentration—lead to changes in the unwinding rate which our model describes quantitatively. Similarly, the free-energy change of melting one NA base pair can be changed by altering solution conditions or by applying a force to the NA molecule. Such a change directly alters α/β in our model, and consequently changes the unwinding rate.

Our simple picture neglects several effects. We ignore unbinding of the helicase from the NA strand. Furthermore, we ignore deformations of the NA strand, such as bending and torsion, and treat the strand as a rigid structure. The helicase is described by forward and backward rates only; we neglect the details of the protein's biochemical states. In addition, we ignore the effects of the NA base sequence on opening; these effects are believed to be weak for helicases [1]. However, recent work by Kafri, Lubensky, and Nelson [22] shows that a motor protein which translocates on a random track can show interesting behavior near the stall force.

The simplified structure of this model means it may be useful in other situations where two nonequilibrium degrees of freedom interact in a biological system. For example, two motor proteins which walk on a microtubule may affect each other's motion. As mentioned above, our work is a generalization of the work of Peskin *et al.* to include an arbitrary interaction potential [17]. This generalization may be relevant to the problem originally addressed in Ref. [17]—the force production by a polymerizing filament. Introducing a potential (which describes the interaction between the growing filament tip and the obstacle against which the polymer pushes) affects the polymerization speed and the force-velocity relation of the filament.

ACKNOWLEDGMENTS

We thank D. Lubensky, T. Perkins, and J. Prost for helpful discussions. M.D.B. acknowledges support from the VIGRE program of the NSF.

APPENDIX A: ESTIMATING THE NA OPENING RATE

Here we estimate the DNA opening rate α from experiments on short hairpins. Bonnet *et al.* measured a rate $k \approx 3000\ s^{-1}$ for the cooperative opening of a 5-bp hairpin loop at room temperature (300 K) [23]. We assume that spontaneous opening of a short hairpin occurs like a zipper from one of the ends and neglect the opening by a fluctuation in the center of the DNA. This assumption is valid for temperatures well below the DNA melting temperature. Suppose that the 5-bp hairpin loop has probability P_i to be in state $i = 0, 1, \ldots, 5$, where i denotes the number of opened base pairs. Transitions between the states satisfy

$$\frac{dP_i}{dt} = \begin{cases} -\alpha P_0 + \beta P_1, & i = 0, \\ -(\alpha+\beta)P_i + \alpha P_{i-1} + \beta P_{i+1}, & i = 1,2,3 \\ -(\alpha+\beta)P_4 + \alpha P_3, & i = 4. \end{cases} \tag{A1}$$

Closing is impossible in the 0 state, which determines the first line of Eq. (A1). We assume that full opening is irre-

versible: the open hairpin (state 5) cannot close again. This assumption is consistent with the experimental observation that the closing rate of a hairpin is orders-of-magnitude slower than its opening rate [23].

After a relaxation time, the Markov process for $i=0,\ldots,4$ reaches a nonequilibrium steady state with $dP_i/dt=0$ and current $J=\alpha P_4$. We use the steady-state condition to solve for the P_i in terms of P_4:

$$P_3 = P_4(1+s^{-1}),$$

$$P_2 = P_4(1+s^{-1}+s^{-2}),$$

$$P_1 = P_4(1+s^{-1}+s^{-2}+s^{-3}),$$

$$P_0 = P_4(1+s^{-1}+s^{-2}+s^{-3}+s^{-4}), \tag{A2}$$

where $s=\alpha/\beta$. The irreversible opening rate of the hairpin is $k=J/\Sigma_{i=0}^{4}P_i$. Therefore,

$$k = \alpha\frac{s^4}{1+2s+3s^2+4s^3+5s^4}. \tag{A3}$$

Substituting $k=3000\ \mathrm{s}^{-1}$ and $s=1/7$ into Eq. (A3) gives the estimate $\alpha\simeq 10^7\ \mathrm{s}^{-1}$. This estimate can be compared with theoretical estimates of the base-pair opening rate α, which range from $10^5\ \mathrm{s}^{-1}$ to $10^6\ \mathrm{s}^{-1}$ [24,25]. Although the spontaneous opening rate is rapid, the closing rate β is approximately 7 times larger—a long DNA molecule tends, on average, to close. Under these conditions, net DNA unwinding requires energy input—for example, from a helicase.

APPENDIX B: TWO-STATE MODEL

In the bulk of this paper, we represent helicase motion only by the rates k^+ and k^- of forward and backward stepping along the NA. Here we discuss a minimal model of helicase motion which takes into account the nonequilibrium nature of this process. Many helicases share features of motion generation with other ATP-consuming motor proteins; thus helicases can be discussed in the same general framework. The model we discuss here is a discrete version of a simple model for motor proteins which hydrolyze ATP to move along a polar track [26–28].

The helicase PcrA is believed to hydrolyze 1 ATP molecule per single-base step on ssDNA [6,18]. The hydrolysis cycle involves several transitions: an ATP molecule first binds the helicase. In the bound state, the ATP molecule is hydrolyzed into one ADP molecule and an inorganic phosphate (P_i). After the ADP and P_i are released from the helicase, the cycle is complete. Any of these biochemical steps may be associated with a conformational change of the protein. Crystal structures of a PcrA/DNA complex have identified two different conformations, corresponding to the ATP-bound and P_i-bound protein [4].

We assume that the protein interacts with the ssNA in two different states *A* and *B*, and biochemical transitions shift the protein between the states. (More distinct biochemical states are possible and could be included in the description.) Because the two states have different conformations, the energy of interaction between the helicase and NA is different in the two states. We neglect NA sequence variation and assume the interaction between the helicase and NA is the same if shifted by one base. Therefore the interaction potential is periodic.

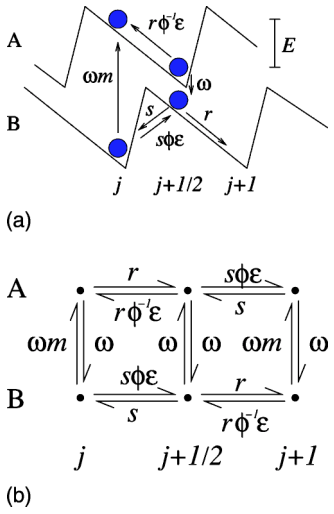

FIG. 6. Schematic of a two-state model for mechanochemical energy transduction. (a) Two-state model characterized by two periodic energy profiles. (b) Discrete version of the two-state model. At each site, two states *A* and *B* are distinguished. Substates are indexed by j and $j+1/2$. For details see text.

Here we consider a discrete version of this two-state model. Each interaction potential is described by two discrete substates per potential period. One potential period corresponds to the helicase step size, and the substates are indexed by j and $j+1/2$. The potential depth is denoted by E, and we consider the possibility of an applied external force F. We use units where one period of the potential has length one and energies are measured in units of k_BT. The probabilities of finding the helicase in a given substate at a given position are P_j^A, $P_{j+1/2}^A$, P_j^B, and $P_{j+1/2}^B$ (Fig. 6).

Two types of transitions between substates occur: (i) transitions between states *A* and *B*, which correspond to a change in potential and (ii) transitions between substates j and $j+1/2$, which correspond to the relaxation (toward a minimum in free energy) that occurs within a chemical state. In our parametrization, transitions between P_j^A and $P_{j+1/2}^A$ occur at forward rate r and backward rate $re^{-E+F/2}$ and between P_j^B and $P_{j+1/2}^B$ at forward rate $se^{-E-F/2}$ and backward rate s. The potentials are assumed to be offset and identical, so the transitions between $P_{j+1/2}^B$ and P_{j+1}^B occur at forward rate r and backward rate $re^{-E+F/2}$ and between $P_{j+1/2}^A$ and P_{j+1}^A at forward rate $se^{-E-F/2}$ and backward rate s (Fig. 6).

Transitions from P_j^B to P_j^A occur at rate $\omega e^{\mu-2E}$ and the reverse transitions at rate ω. The free-energy difference between *A* and *B* at point j is $2E$. The chemical potential μ represents the free energy released from hydrolysis of one ATP molecule; if $\mu=0$, the transition is at equilibrium. The two substates at $j+1/2$ are assumed to be at the same energy, and transitions occur at rate ω in both directions. For conve-

nience we introduce the symbols $\epsilon = e^{-E}$, $\phi = e^{-F/2}$, and $m = e^{\mu - 2E}$. The probability currents are defined by

$$J_j^A = rP_j^A - r\epsilon\phi^{-1}P_{j+1/2}^A,$$

$$J_j^B = s\epsilon\phi P_j^B - sP_{j+1/2}^B,$$

$$J_{j+1/2}^A = s\epsilon\phi P_{j+1/2}^A - sP_{j+1}^A,$$

$$J_{j+1/2}^B = rP_{j+1/2}^B - r\epsilon\phi^{-1}P_{j+1}^B. \tag{B1}$$

The individual probabilities obey

$$\frac{dP_j^A}{dt} = -J_j^A + J_{j-1/2}^A - \omega P_j^A + \omega m P_j^B,$$

$$\frac{dP_j^B}{dt} = -J_j^B + J_{j-1/2}^B + \omega P_j^A - \omega m P_j^B,$$

$$\frac{dP_{j+1/2}^A}{dt} = -J_{j+1/2}^A + J_j^A - \omega P_{j+1/2}^A + \omega P_{j+1/2}^B,$$

$$\frac{dP_{j+1/2}^B}{dt} = -J_{j+1/2}^B + J_j^B + \omega P_{j+1/2}^A - \omega P_{j+1/2}^B. \tag{B2}$$

Steady-state properties

We consider the steady state where the rates of change of the probabilities in Eq. (B2) vanish. The probabilities P^A, $P_{1/2}^A$, P^B, and $P_{1/2}^B$ are independent of j and satisfy

$$\begin{bmatrix} -(r+s+\omega) & \omega m & \epsilon(r\phi^{-1}+s\phi) & 0 \\ \omega & -[\epsilon(r\phi^{-1}+s\phi)+\omega m] & 0 & (r+s) \\ (r+s) & 0 & -[\epsilon(r\phi^{-1}+s\phi)+\omega] & \omega \\ 0 & \epsilon(r\phi^{-1}+s\phi) & \omega & -(r+s+\omega) \end{bmatrix} \begin{bmatrix} P^A \\ P^B \\ P_{1/2}^A \\ P_{1/2}^B \end{bmatrix} = 0. \tag{B3}$$

The null space of this matrix determines the steady-state probability vector, which we normalize so that $P^A + P^B + P_{1/2}^A + P_{1/2}^B = 1$. The total steady-state current is

$$J = J^A + J^B = rP^A + s\epsilon\phi P^B - r\epsilon\phi^{-1}P_{1/2}^A - sP_{1/2}^B. \tag{B4}$$

For the special case of no applied force ($\phi = 1$), the current is

$$J_{\phi=1} = \frac{\omega(r-s)(m-\epsilon^2)}{(r+s)(1+m+3\epsilon+m\epsilon+2\epsilon^2)+\omega(1+3m+3\epsilon+m\epsilon)},$$

$$= \frac{\omega e^{-2E}(r-s)(e^{\mu}-1)}{(r+s)(1+e^{\mu-2E}+3e^{-E}+e^{\mu-3E}+2e^{-2E})+\omega(1+3e^{\mu-2E}+3e^{-E}+e^{\mu-3E})}. \tag{B5}$$

The sign of the current is given by the product $(r-s)(e^{\mu}-1)$. The conditions for zero current are as expected: if $r=s$, then the potentials are symmetric. Thus the current must be zero. Similarly, if the chemical potential from the fuel is $\mu = 0$, then detailed balance must be satisfied and there is no motion. It is useful to give an approximate expression for the current in the case $E \gg 1$ and $\mu - 2E \gg 1$. Then the terms proportional to $e^{\mu-2E}$ dominate in the denominator, and the current is approximately

$$J_{\phi=1} \approx \frac{\omega(r-s)(1-e^{-\mu})}{r+s+3\omega}. \tag{B6}$$

Effective hopping rates

Summing over the probabilities of different states in a given period j we obtain an effective hopping model. In this averaged model, the system has probability P_j to be at site j; effective forward and backward hopping rates k^+ and k^- connect adjacent sites. This effective system is described by the equation

$$\frac{dP_j}{dt} = -(k^+ + k^-)P_j + k^+P_{j-1} + k^-P_{j+1}. \tag{B7}$$

At steady state, we can reduce the full model in Eq. (B2) to this effective description. Summing Eq. (B2) we find

$$\frac{d}{dt}(P_j^A + P_j^B + P_{j+1/2}^A + P_{j+1/2}^B) = J_{j-1/2}^A + J_{j-1/2}^B - J_{j+1/2}^A - J_{j+1/2}^B$$

$$= J_{j-1/2} - J_{j+1/2}, \tag{B8}$$

where we have defined the current

$$J_{j-1/2} = s\epsilon\phi P^A_{j-1/2} + rP^B_{j-1/2} - sP^A_j - r\epsilon\phi^{-1}P^B_j. \quad \text{(B9)}$$

This formula can be rewritten in terms of P^A_j and P^A_{j-1}:

$$J_{j-1/2} = \left[s\epsilon\phi\frac{P^A_{j-1/2}}{P^A_{j-1}} + r\frac{P^B_{j-1/2}}{P^A_{j-1}} \right] P^A_{j-1} - \left[s + r\epsilon\phi^{-1}\frac{P^B_j}{P^A_j} \right] P^A_j. \quad \text{(B10)}$$

Thus we obtain

$$\begin{aligned}\frac{dP_j}{dt} = &-\left(s + r\epsilon\phi^{-1}\frac{P^B_j}{P^A_j} + s\epsilon\phi\frac{P^A_{j+1/2}}{P^A_j} + r\frac{P^B_{j+1/2}}{P^A_j} \right) P_j \\ &+ \left(s\epsilon\phi\frac{P^A_{j-1/2}}{P^A_{j-1}} + r\frac{P^B_{j-1/2}}{P^A_{j-1}} \right) P_{j-1} \\ &+ \left(s + r\epsilon\phi^{-1}\frac{P^B_{j+1}}{P^A_{j+1}} \right) P_{j+1}. \quad \text{(B11)}\end{aligned}$$

At steady state, the probabilities are independent of j, so we can drop the subscripts. Thus we can read off the effective hopping rates

$$k^- = s + r\epsilon\phi^{-1}\frac{P^B}{P^A} = \frac{sP^A + r\epsilon\phi^{-1}P^B}{P^A},$$

$$k^+ = s\epsilon\phi\frac{P^A_{1/2}}{P^A} + r\frac{P^B_{1/2}}{P^A} = \frac{s\epsilon\phi P^A_{1/2} + rP^B_{1/2}}{P^A}. \quad \text{(B12)}$$

We give full expressions for the hopping rates in the case of zero force ($\phi=1$):

$$k^+_{\phi=1} = \frac{\epsilon^2[(r+s)^2 + s\omega] + \epsilon[r^2 + s^2m + sm(r+\omega) + r(\omega+s)] + r\omega m}{(r+s)(1+m+3\epsilon+m\epsilon+2\epsilon^2) + \omega(1+3m+3\epsilon+m\epsilon)},$$

$$k^-_{\phi=1} = \frac{\epsilon^2[(r+s)^2 + r\omega] + \epsilon[r^2 + s^2m + sm(r+\omega) + r(\omega+s)] + s\omega m}{(r+s)(1+m+3\epsilon+m\epsilon+2\epsilon^2) + \omega(1+3m+3\epsilon+m\epsilon)}. \quad \text{(B13)}$$

Note that, as expected, subtracting these rates we recover the expression for the current in Eq. (B5): $J_{\phi=1} = k^+_{\phi=1} - k^-_{\phi=1}$.

Ratio of hopping rates with applied force

An important quantity is the ratio of forward and backward hopping rates

$$\frac{k^+}{k^-} = \frac{sP^A + r\epsilon\phi^{-1}P^B}{s\epsilon\phi P^A_{1/2} + rP^B_{1/2}},$$

$$= \frac{e^{\mu-E}(r+s)r\omega\phi^2 + e^{\mu-2E}(r+s)s(r+s+\omega)\phi^2 + O(1)}{e^{\mu-E}(r+s)s\omega\phi^2 + e^{\mu-2E}s(r+s+\omega)(r\phi+s\phi^3) + O(1)}, \quad \text{(B14)}$$

which becomes a detailed balance relation if $\mu=0$. Note in particular that if $F=0$ and $\mu=0$, this ratio is 1, as expected, since in the absence of a chemical potential and applied force the helicase must undergo an unbiased random walk.

We wish to take the opposite limit: the chemical potential of ATP hydrolysis is approximately 20 k_BT. Thus we assume $\mu \gg 1$ so that terms not proportional to e^μ are negligible. For the remainder of this appendix, all expressions are approximations valid for large μ. In this limit, the ratio becomes

$$\frac{k^+}{k^-} \approx \frac{r + e^{-E}\frac{s}{\omega}(r+s+\omega)}{s + e^{-E}\frac{s}{\omega}\frac{r+s+\omega}{r+s}(re^{F/2} + se^{-F/2})}. \quad \text{(B15)}$$

For large positive F (a force opposing the helicase motion), the second term in the denominator dominates and we have

$$\frac{k^+}{k^-} \approx \left(r + e^{-E}\frac{s}{\omega}(r+s+\omega) \right) \frac{\omega(r+s)e^E}{rs(r+s+\omega)} e^{-F/2},$$

$$= \frac{k^+_0}{k^-_0} e^{-F/2}. \quad \text{(B16)}$$

In this limit, the applied force modifies the ratio of forward-backward helicase hopping rates with an exponential, detailed-balance-like relation. A linear interaction potential will have the same effect on the ratio of k^+ to k^-.

[1] T. M. Lohman and K. P. Bjornson, Annu. Rev. Biochem. **65**, 169 (1996).
[2] P. H. von Hippel and E. Delagoutte, Cell **104**, 177 (2001).
[3] M. R. Singleton and D. B. Wigley, J. Bacteriol. **184**, 1819 (2002).
[4] S. S. Velankar, P. Soultanas, M. S. Dillingham, H. S. Subramanya, and D. B. Wigley, Cell **97**, 75 (1999).
[5] P. Soultanas, M. S. Dillingham, P. Wiley, M. R. Webb, and D. B. Wigley, EMBO J. **19**, 3799 (2000).
[6] M. S. Dillingham, D. B. Wigley, and M. R. Webb, Biochemistry **39**, 205 (2000).
[7] K. M. Dohoney and J. Gelles, Nature (London) **409**, 370 (2001).
[8] P. R. Bianco, L. R. Brewer, M. Corzett, R. Balhorn, Y. Yeh, S. C. Kowalczykowski, and R. J. Baskin, Nature (London) **409**, 374 (2001).
[9] T. T. Perkins, H. W. Li, R. V. Dalal, J. Gelles, and S. M. Block, Biophys. J. **86**, 1640 (2004).
[10] E. Nudler, A. Goldfarb, and M. Kashlev, Science **265**, 793 (1994).
[11] S. M. Uptain, C. M. Kane, and M. J. Camberlin, Annu. Rev. Biochem. **66**, 117 (1997).
[12] C. Doering, B. Ermentrout, and G. Oster, Biophys. J. **69**, 2256 (1995).
[13] Y. Z. Chen, D. Mi, H.-S. Song, and X.-J. Wang, Phys. Rev. E **56**, 919 (1997).
[14] S. M. Bhattacharjee and F. Seno, J. Phys. A **36**, L181 (2003).
[15] M. D. Betterton and F. Jülicher, Phys. Rev. Lett. **91**, 258103 (2003).
[16] S. Nonin, J.-L. Leroy, and M. Guéron, Biochemistry **34**, 10652 (1995).
[17] C. S. Peskin, G. M. Odell, and G. F. Oster, Biophys. J. **65**, 316 (1993).
[18] M. S. Dillingham, D. B. Wigley, and M. R. Webb, Biochemistry **41**, 643 (2002).
[19] D. E. Kim, M. Narayan, and S. S. Patel, J. Mol. Biol. **321**, 807 (2002).
[20] A. Henn, O. Medalia, H. P. Shi, M. Steinberg, F. Franceschi, and I. Sagi, Proc. Natl. Acad. Sci. U.S.A. **98**, 5007 (2001).
[21] T. Ha, I. Rasnik, W. Cheng, H. P. Babcock, G. H. Gauss, T. M. Lohman, and S. Chu, Nature (London) **419**, 638 (2002).
[22] Y. Kafri, D. K. Lubensky, and D. R. Nelson, Biophys. J. **86**, 3373 (2004).
[23] G. Bonnet, O. Krichevsky, and A. Libchaber, Proc. Natl. Acad. Sci. U.S.A. **95**, 8602 (1998).
[24] Y. Z. Chen, W. Zhuang, and E. W. Prohofsky, J. Biomol. Struct. Dyn. **10**, 415 (1992).
[25] M. D. Frank-Kamenetskii, Phys. Rep. **288**, 13 (1997).
[26] C. Peskin, B. Ermentrout, and G. Oster, in *Cell Mechanics and Cellular Engineering*, edited by V. C. Mow, F. Guilak, R. Tran-Son-Tay, and R. Hochmuth, (Springer-Verlag, New York, 1994), pp. 479–489.
[27] F. Jülicher, A. Ajdari, and J. Prost, Rev. Mod. Phys. **69**, 1269 (1997).
[28] R. D. Astumian, Science **276**, 917 (1997).